

MIT Open Access Articles

Low-cost, single-mode diode-pumped Cr:Colquiriite lasers

The MIT Faculty has made this article openly available. **Please share** how this access benefits you. Your story matters.

Citation: Demirbas, Umit, Duo Li, Jonathan R. Birge, Alphan Sennaroglu, Gale S. Petrich, Leslie A. Kolodziejski, Franz X. Kaertner, and James G. Fujimoto. "Low-Cost, Single-Mode Diode-Pumped Cr:Colquiriite Lasers." *Optics Express* 17, no. 16 (August 3, 2009): 14374. © 2009 Optical Society of America

As Published: <http://dx.doi.org/10.1364/OE.17.014374>

Publisher: Optical Society of America

Persistent URL: <http://hdl.handle.net/1721.1/86134>

Version: Final published version: final published article, as it appeared in a journal, conference proceedings, or other formally published context

Terms of Use: Article is made available in accordance with the publisher's policy and may be subject to US copyright law. Please refer to the publisher's site for terms of use.



Low-cost, single-mode diode-pumped Cr:Colquiriite lasers

Umit Demirbas,¹ Duo Li,¹ Jonathan R. Birge,¹ Alphan Sennaroglu,^{1,2} Gale S. Petrich,¹ Leslie A. Kolodziejski,¹ Franz X. Kärtner,¹ and James G. Fujimoto¹

¹Department of Electrical Engineering and Computer Science and Research Laboratory of Electronics, Massachusetts Institute of Technology, Cambridge, Massachusetts 02139, USA

²Laser Research Laboratory, Department of Physics, Koç University, Rumelifeneri, Sariyer, 34450 Istanbul, Turkey
*umit@mit.edu and jgf@mit.edu

Abstract: We present three Cr³⁺:Colquiriite lasers as low-cost alternatives to Ti:Sapphire laser technology. Single-mode laser diodes, which cost only \$150 each, were used as pump sources. In cw operation, with ~520 mW of absorbed pump power, up to 257, 269 and 266 mW of output power and slope efficiencies of 53%, 62% and 54% were demonstrated for Cr:LiSAF, Cr:LiSGaF and Cr:LiCAF, respectively. Record cw tuning ranges from 782 to 1042 nm for Cr:LiSAF, 777 to 977 nm for Cr:LiSGaF, and 754 to 871 nm for Cr:LiCAF were demonstrated. In cw mode-locking experiments using semiconductor saturable absorber mirrors at 800 and 850 nm, Cr:Colquiriite lasers produced ~50-100 fs pulses with ~1-2.5 nJ pulse energies at ~100 MHz repetition rate. Electrical-to-optical conversion efficiencies of 8% in mode-locked operation and 12% in cw operation were achieved.

©2009 Optical Society of America

OCIS codes: (140.3460) Lasers; (140.4050) Mode-locked lasers; (140.3580) Lasers, solid-state; (140.3480) Lasers, diode pumped; (140.3600) Lasers, tunable; (140.5680) Rare earth and transition metal solid-state lasers.

References and links

1. R. Ell, U. Morgner, F. X. Kärtner, J. G. Fujimoto, E. P. Ippen, V. Scheuer, G. Angelow, and T. Tschudi, "Generation of 5 fs pulses and octave-spanning spectra directly from a Ti:sapphire laser," *Opt. Lett.* **26**, 373-375 (2001).
2. S. A. Payne, L. L. Chase, L. K. Smith, W. L. Kway, and H. W. Newkirk, "Laser performance of LiSAIF₆:Cr³⁺," *J. Appl. Phys.* **66**, 1051-1056 (1989).
3. L. K. Smith, S. A. Payne, W. L. Kway, L. L. Chase, and B. H. T. Chai, "Investigation of the laser properties of Cr³⁺:LiSrGaF₆," *IEEE J. Quantum Electron.* **28**, 2612-2618 (1992).
4. S. A. Payne, L. L. Chase, H. W. Newkirk, L. K. Smith, and W. F. Krupke, "LiCaAlF₆:Cr³⁺ a promising new solid-state laser material," *IEEE J. Quantum Electron.* **24**, 2243-2252 (1988).
5. U. Keller, K. J. Weingarten, F. X. Kärtner, D. Kopf, B. Braun, I. D. Jung, R. Fluck, C. Hönninger, N. Matuschek, and J. A. der Au, "Semiconductor saturable absorber mirrors (SESAM's) for femtosecond to nanosecond pulse generation in solid-state lasers," *IEEE J. Sel. Top. Quantum Electron.* **2**, 435-453 (1996).
6. S. Tsuda, W. H. Knox, S. T. Cundiff, W. Y. Jan, and J. E. Cunningham, "Mode-locking ultrafast solid-state lasers with saturable Bragg reflectors," *IEEE Sel. Top. Quantum Electron.* **2**, 454-464 (1996).
7. M. Stalder, M. Bass, and B. H. T. Chai, "Thermal quenching of fluorescence in chromium-doped fluoride laser crystals," *J. Opt. Soc. Am. B* **9**, 2271-2273 (1992).
8. M. Stalder, B. H. T. Chai, and M. Bass, "Flashlamp pumped Cr:LiSrAlF₆ laser," *Appl. Phys. Lett.* **58**, 216-218 (1991).
9. I. T. Sorokina, E. Sorokin, E. Wintner, A. Cassanho, H. P. Jenssen, and M. A. Noginov, "Efficient cw TEM₀₀ and femtosecond Kerr-lens modelocked Cr:LiSrGaF laser," *Optics Lett.* **21**, 204-206 (1996).
10. S. Uemura, and K. Torizuka, "Generation of 10 fs pulses from a diode-pumped Kerr-lens mode-locked Cr:LiSAF laser," *Jpn. J. Appl. Phys.* **39**, 3472-3473 (2000).
11. I. T. Sorokina, E. Sorokin, E. Wintner, A. Cassanho, H. P. Jenssen, and R. Szpoc, "14-fs pulse generation in Kerr-lens mode-locked prismless Cr:LiSGaF and Cr:LiSAF lasers: observation of pulse self-frequency shift," *Opt. Lett.* **22**, 1716-1718 (1997).
12. P. Wagenblast, U. Morgner, F. Grawert, V. Scheuer, G. Angelow, M. J. Lederer, and F. X. Kärtner, "Generation of sub-10-fs pulses from a Kerr-lens modelocked Cr³⁺:LiCAF laser oscillator using third order dispersion compensating double chirped mirrors," *Opt. Lett.* **27**, 1726-1729 (2002).

13. E. Sorokin, "Solid-state materials for few-cycle pulse generation and amplification," in *Few-cycle laser pulse generation and its applications*, F. X. Kärtner, ed. (Springer-Verlag, Berlin, 2004), pp. 3-71.
14. F. Druon, F. Balembois, and P. Georges, "New laser crystals for the generation of ultrashort pulses," *Comptes Rendus Physique* **8**, 153-164 (2007).
15. A. Sanchez, R. E. Fahey, A. J. Strauss, and R. L. Aggarwal, "Room-temperature continuous-wave operation of a Ti:Al₂O₃ laser," *Opt. Lett.* **11**, 363-364 (1986).
16. J. K. Jabczynski, W. Zendzian, Z. Mierczyk, and Z. Frukacz, "Chromium-doped LiCAF laser passively Q switched with a V³⁺:YAG crystal," *Appl. Opt.* **40**, 6638-6645 (2001).
17. L. J. Atherton, S. A. Payne, and C. D. Brandle, "Oxide and fluoride laser crystals," *Annual Review of Materials Science* **23**, 453-502 (1993).
18. J. M. Eichenholz, and M. Richardson, "Measurement of thermal lensing in Cr³⁺-doped colquiriites," *IEEE J. Quantum Electron.* **34**, 910-919 (1998).
19. D. Kopf, K. J. Weingarten, G. Zhang, M. Moser, M. A. Emanuel, R. J. Beach, J. A. Skidmore, and U. Keller, "High-average-power diode-pumped femtosecond Cr:LiSAF lasers," *Appl. Phys. B* **65**, 235-243 (1997).
20. U. Demirbas, A. Sennaroglu, A. Benedick, A. Siddiqui, F. X. Kärtner, and J. G. Fujimoto, "Diode-pumped, high-average power femtosecond Cr³⁺:LiCAF laser," *Opt. Lett.* **32**, 3309-3311 (2007).
21. U. Demirbas, A. Sennaroglu, F. X. Kärtner, and J. G. Fujimoto, "Comparative investigation of diode pumping for continuous-wave and mode-locked Cr³⁺:LiCAF lasers," *J. Opt. Soc. Am. B* **26**, 64-79 (2009).
22. P. M. W. French, R. Mellish, J. R. Taylor, P. J. Delfyett, and L. T. Florez, "Mode-locked all-solid-state diode-pumped Cr:LiSAF Laser," *Opt. Lett.* **18**, 1934-1936 (1993).
23. R. P. Prasankumar, Y. Hirakawa, A. M. J. Kowalevicz, F. X. Kärtner, J. G. Fujitimo, and W. H. Knox, "An extended cavity femtosecond Cr:LiSAF laser pumped by low cost diode lasers," *Opt. Express* **11**, 1265-1269 (2003).
24. U. Demirbas, A. Sennaroglu, F. X. Kärtner, and J. G. Fujimoto, "Highly efficient, low-cost femtosecond Cr³⁺:LiCAF laser pumped by single-mode diodes," *Opt. Lett.* **33**, 590-592 (2008).
25. R. Scheps, J. F. Myers, H. B. Serreze, A. Rosenberg, R. C. Morris, and M. Long, "Diode-pumped Cr:LiSrAlF₆ laser," *Opt. Lett.* **16**, 820-822 (1991).
26. G. J. Valentine, J. M. Hopkins, P. Loza-Alvarez, G. T. Kennedy, W. Sibbett, D. Burns, and A. Valster, "Ultralow-pump-threshold, femtosecond Cr³⁺:LiSrAlF₆ laser pumped by a single narrow-stripe AlGaInP laser diode," *Opt. Lett.* **22**, 1639-1641 (1997).
27. S. Tsuda, W. H. Knox, and S. T. Cundiff, "High efficiency diode pumping of a saturable Bragg reflector-mode-locked Cr:LiSAF femtosecond laser," *Appl. Phys. Lett.* **69**, 1538-1540 (1996).
28. J. M. Hopkins, G. J. Valentine, W. Sibbett, J. A. der Au, F. Morier-Genoud, U. Keller, and A. Valster, "Efficient, low-noise, SESAM-based femtosecond Cr³⁺:LiSrAlF₆ laser," *Opt. Comm.* **154**, 54-58 (1998).
29. S. Sakadžić, U. Demirbas, T. R. Mempel, A. Moore, S. Ruvinskaya, D. A. Boas, A. Sennaroglu, F. X. Kärtner, and J. G. Fujimoto, "Multi-photon microscopy with a low-cost and highly efficient Cr:LiCAF laser," *Opt. Express* **16**, 20848-20863 (2008).
30. U. Demirbas, A. Sennaroglu, F. X. Kärtner, and J. G. Fujimoto, "Generation of 15 nJ pulses from a highly efficient, low-cost multipass-cavity Cr³⁺:LiCAF laser," *Opt. Lett.* **34**, 497-499 (2009).
31. D. Kopf, A. Prasad, G. Zhang, M. Moser, and U. Keller, "Broadly tunable femtosecond Cr:LiSAF laser," *Opt. Lett.* **22**, 621-623 (1997).
32. R. Mellish, S. C. W. Hyde, N. P. Barry, R. Jones, P. M. W. French, J. R. Taylor, C. J. vanderPoel, and A. Valster, "All-solid-state diode-pumped Cr:LiSAF femtosecond oscillator and regenerative amplifier," *Appl. Phys. B* **65**, 221-226 (1997).
33. A. Robertson, R. Knappe, and R. Wallenstein, "Diode-pumped broadly tunable (809-910 nm) femtosecond Cr:LiSAF laser," *Opt. Comm.* **147**, 294-298 (1998).
34. S. N. Tandon, J. T. Gopinath, H. M. Shen, G. S. Petrich, L. A. Kolodziejcki, F. X. Kärtner, and E. P. Ippen, "Large-area broadband saturable Bragg reflectors by use of oxidized AlAs," *Optics letters* **29**, 2551-2553 (2004).
35. D. H. Sutter, L. Gallmann, N. Matuschek, F. Morier-Genoud, V. Scheuer, G. Angelow, T. Tschudi, G. Steinmeyer, and U. Keller, "Sub-6-fs pulses from a SESAM-assisted Kerr-lens mode-locked Ti:sapphire laser: at the frontiers of ultrashort pulse generation," *Appl. Phys. B*, 631-633 (2000).

1. Introduction

Among solid-state vibronic lasers, Ti:Sapphire has the broadest tuning range (660-1180 nm), and can directly generate sub-5-fs pulses [1]. However, because direct diode pumping is not currently possible, Ti:Sapphire lasers are typically pumped by frequency-doubled diode-pumped neodymium lasers, which are bulky and cost \$50-100k, making the overall system cost high and limiting wide-spread use.

Cr³⁺-doped colquiriite crystals such as Cr³⁺:LiSAF [2], Cr³⁺:LiSGaF [3], and Cr³⁺:LiCAF [4] are an attractive alternative to Ti:Sapphire. They provide broadly tunable operation around 800 nm, enabling the generation of pulses as short as ~10-fs (Table 1). Their absorption bands are red shifted to ~650 nm, enabling direct diode pumping with low-cost diode lasers,

significantly reducing the total cost of the laser system. Other advantages of Cr:Colquiriites are their low lasing threshold (~ 10 mW) and high intrinsic slope efficiencies ($>50\%$), enabling efficient laser operation with electrical-to-optical conversion efficiencies exceeding 10%. Unfortunately, compared to Ti:Sapphire, Cr:Colquiriites have low emission cross sections (σ_{em}), low third-order nonlinearity (n_2), and they have a significant amount of excited state absorption. The lower emission cross section results in lower small signal gain, requiring low-loss optics (especially for Cr:LiCAF). The low nonlinearity makes Kerr-lens mode-locking (KLM) difficult, especially for commercial systems. Nevertheless, saturable absorber mirrors (SESAMs) [5], also known as saturable Bragg reflectors (SBRs) [6], can be used to obtain stable, turn-key mode-locked operation. However, the bandwidth limitation of standard SESAMs/SBRs limits pulsewidths to the ~ 50 fs level and restricts tunability to ranges of a few tens of nm.

Table 1. Comparison of the spectroscopic and laser parameters of the Ti:Sapphire, Cr:LiSAF, Cr:LiSGaF, and Cr:LiCAF gain media. *Denotes the results obtained in this work. $T_{1/2}$ is the temperature at which the fluorescence lifetime (τ_f) drops to half of the radiative lifetime (τ_{rad}) [7].

Gain Medium	Ti ³⁺ :Al ₂ O ₃ (Ti:Sapphire)	Cr ³⁺ :LiSrAlF ₆ (Cr:LiSAF)	Cr ³⁺ : LiSrGaF ₆ (Cr:LiSGaF)	Cr ³⁺ :LiCaAlF ₆ (Cr:LiCAF)
Tuning range [nm]	660-1180	780-1010 [8] 782-1042*	785-935 [9] 777-977*	720-840 [4] 754-871*
Demonstrated shortest pulse length [fs]	~ 5 [1]	10 [10]	14 [11]	9 [12]
Nonlinear refractive index (n_2) [$\times 10^{-16}$ cm ² /W]	3.2 [13]	0.8 [13]	1.2 [13]	0.4 [13]
Peak emission cross section (σ_{em}) [$\times 10^{-20}$ cm ²]	41 [14]	4.8 [14]	3.3 [3]	1.3 [14]
Room-temperature fluorescence lifetime (τ_f) [μ s]	3.2 [14]	67 [14]	88 [3]	175 [14]
$\sigma_{em}\tau_f$ [μ s $\times 10^{-20}$ cm ²]	131 [14]	322 [14]	290 [14]	228 [14]
Intrinsic slope efficiency [%]	64 [15]	53 [2], 54*	52% [3], 60*	67 [4], 69*
Relative strength of excited-state absorption (σ_{esa}/σ_{em})	~ 0	0.33 [16]	0.33 [3]	0.18 [16]
Thermal conductivity [W/K.m]	28 [17]	3.1 [17]	3.6 [13]	5.1 [17]
$T_{1/2}$, $\tau_f(T_{1/2})=0.5\tau_{rad}$ [C]	~ 100	69 [7]	88 [18]	190-255 [7, 18]
Auger Rate [10^{16} cm ³ /s]	-	6.5 [16]	6.5 [16]	1.65 [16]

Cr:Colquiriites can be pumped by laser diode arrays [19], broad-stripe single-emitter diodes [20-22], and single transverse-mode laser diodes [21, 23, 24]. Although higher output powers are possible using multimode diodes [19-22], single-mode diode-pumping provides lower cost, ease of operation, better mode-matching, significantly lower lasing thresholds, reduced thermal effects, and higher efficiencies [21, 24]. Moreover, for single-mode diode-pumping, no cooling is needed for the pump diodes or laser crystal, enabling compact, portable systems. Single-mode diode-pumping was first applied to cw and mode-locked Cr:Colquiriites by Scheps et al. [25] and Valentine et al. [26], respectively. These early studies suggested the possibility of low-cost and efficient diode-pumped femtosecond Cr:Colquiriites lasers [27, 28]. However, to our knowledge, until recently, single-mode diode-pumping was applied only to Cr:LiSAF and cw powers and output energies were limited to about ~ 50 mW, and 0.75 nJ, respectively. Previous studies focused on Cr:LiSAF, since it has the highest gain cross section and broadest tunability. Recently, we described a single-mode diode-pumped Cr:LiCAF laser producing 280 mW of cw output and 1.4 nJ of mode-locked pulse energy [24]. Electrical-to-optical conversion efficiencies were 7.8% in mode-locked and 12.2% in cw operation [24]. These improvements were enabled by recent advances in crystal growth, mirror coating, and laser diodes. This study [24] provided a motivation to extend the earlier work to other Cr:Colquiriite materials.

In this paper, we investigate single-mode diode-pumped Cr:LiSAF, Cr:LiSGaF, and Cr:LiCAF lasers. In cw operation, using ~ 520 mW of absorbed pump power, up to 257, 269 and 266 mW of output power and slope efficiencies of 53%, 62% and 54% were demonstrated for Cr:LiSAF, Cr:LiSGaF and Cr:LiCAF lasers, respectively. Using birefringent filters or fused silica prisms for tuning, we demonstrated record cw tuning ranges for Cr:LiSAF (782-1042 nm), Cr:LiSGaF (777-977 nm), and Cr:LiCAF (754-871 nm). For femtosecond pulse generation, SESAMs/SBRs centered at 800 nm and 850 nm were used to initiate and sustain mode-locking [5, 6]. The SESAM/SBR mode-locked lasers were self-starting, immune to environmental fluctuations and did not require careful cavity alignment, enabling turn-key operation. Typical performance was ~ 50 -100 fs pulses with 1-2.5 nJ pulse energies at ~ 100 MHz repetition rate. To the best of our knowledge, these are the highest average powers and pulse energies that have been obtained from single-mode diode-pumped Cr:Colquiriites. Electrical-to-optical conversion efficiencies up to 12% and 8% were demonstrated for cw and cw mode-locked operation, which we believe, are among the highest efficiencies that have been obtained from femtosecond solid state lasers. The paper is organized as follows: section 2 describes the experimental setup. In section 3 and 4, we present the cw and cw mode-locked lasing results, respectively. Finally, in section 5, we summarize the results and provide a general discussion.

2. Experimental

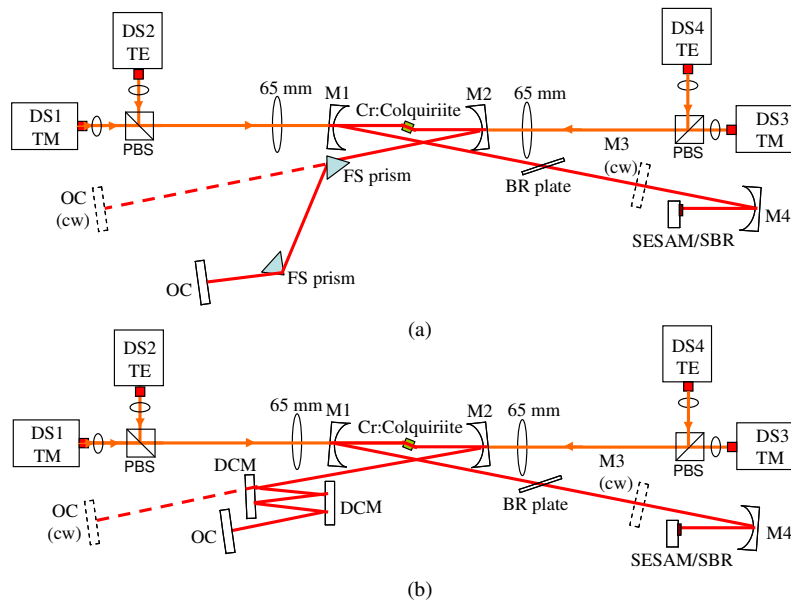


Fig. 1. Schematics of the single-mode diode-pumped Cr³⁺:Colquiriite lasers. In (a), a fused silica (FS) prism pair, and in (b) double chirped mirrors (DCM) were used for dispersion compensation. DS1-DS4: Single-mode pump diodes at 660 nm, PBS: polarizing beam splitting cube, M1-M2: pump mirrors with R= 75 mm, M3: flat high reflector, DCM: flat double-chirped mirrors with ~ -50 to -80 fs² dispersion per bounce, SESAM/SBR: semiconductor saturable absorber mirror / saturable Bragg reflector, BR plate: birefringent plate for tuning. Dashed lines indicate the cw laser cavity.

Figure 1 shows the schematics of the single-mode diode-pumped Cr:Colquiriite lasers, with (a) a fused silica (FS) prism pair and (b) double chirped mirrors (DCMs) for dispersion compensation. The gain was pumped by four, linearly-polarized, $\sim 660 \pm 2$ nm AlGaInP single-mode diodes (DS1-DS4) with circular output, each costing only $\sim \$150$ (VPSL-0660-130-X-5-G, Blue Sky Research). A maximum pump power of ~ 150 -160 mW per diode (above the rated output power of 130 mW) could be obtained by driving at a current of 220 mA (above the rated driving current of 170-210 mA). The electrical-to-optical conversion efficiency was

~25% and water cooling was not required. The output of the diodes was collimated by aspheric lenses ($f = 4.5$ mm) and combined using polarizing beam splitting (PBS) cubes. Two 65-mm focal length lenses focused the pump beams in the Cr:Colquiriite crystals.

Astigmatically-compensated, x-folded laser cavities with two curved pump mirrors (M1 and M2, $R=75$ mm), a flat end mirror (M3), and a flat output coupler (OC) were used. Pump mirrors had high reflectivity from 750 to 850 nm ($R>99.9\%$) and $>95\%$ transmission at the pump wavelength. A long cavity arm length of ~60 cm was used to obtain a beam waist of ~20 μm inside the crystals. The following Brewster-cut Cr:Colquiriite gain media (from VLOC, Inc.) were used: (i) a 5-mm-long, 1.5% Cr-doped Cr:LiSAF crystal which absorbed ~99% and ~72% (0.9 x 80%) of the incident TM and TE polarized pump at ~660 nm, (ii) a 5-mm-long, 3% Cr-doped Cr:LiSGaF crystal [TM and TE absorption = ~99.5% and ~86.5% (0.9 x 96%)], (iii) a 2 mm-long, 10% Cr-doped Cr:LiCAF [TM and TE absorption = ~97.5% and ~84% (0.9 x 93.5%)]. The crystals were cut so that the electric field of the TM polarized light was parallel to the crystal c-axis. All of the crystals were about ~1.5 mm thick and were mounted with indium foil and embedded in a copper holder. Water cooling was not used (except for the data in Fig. 5, where thermal issues were investigated). In the cw tuning experiments, a Brewster-cut fused silica prism or 300-400 μm thick crystal quartz birefringent filters was used to tune the laser wavelength. To cover the full tuning range of Cr:LiSGaF and Cr:LiSAF, another broadband pump mirror set was also used (only for the curves of Cr:LiSGaF and Cr:LiSAF, shown in Fig. 4). These broadband pump mirrors had reflectivity greater than 99.8% from 730 to 1030 nm and $>95\%$ transmission at the pump wavelength.

For mode-locked operation, dispersion compensation was performed by a fused silica (FS) prism pair or by double-chirped mirrors (DCMs) (see Fig. 1). FS prism pairs enabled fine dispersion tuning by varying the prism insertion; however, cavities with prism pairs are more sensitive to cavity misalignment and have a larger footprint. Both commercial (Layertec, GmbH.) and custom designed (designed at MIT and grown by Advanced Thin Films, Inc.) DCMs were used for dispersion compensation. DCMs have improved ease of use and stability, but total cavity dispersion can be adjusted only in discrete increments by varying the number of mirror bounces. The commercial DCMs had a group velocity dispersion (GVD) of ~ -50 \pm 10 fs² per bounce. The custom designed DCMs were optimized for the dispersion of the Cr:LiSAF laser and had a GVD of ~ -80 fs² per bounce. In some experiments, Gires-Tournois interferometer (GTI) mirrors, with a GVD ~ -550 \pm 50 fs² per bounce were also used. The GTI mirrors had limited bandwidth, but high GVD, requiring only 1-2 bounces in order to compensate the cavity dispersion. In mode-locking tuning experiments, a specially designed, 3 mm thick crystal quartz birefringent filter, with the optic axis out of plane was used.

Two different SESAMs/SBRs with low nonsaturable loss (~0.5%) were used to initiate and sustain mode-locking. The first (800 nm SESAM/SBR) had a ~65 nm reflectivity bandwidth centered around 800 nm ($R>99\%$). In this SESAM/SBR design, twenty pairs of $\text{AlAs}/\text{Al}_{0.17}\text{Ga}_{0.83}\text{As}$ quarter-wave layers were used in a Bragg mirror stack and five layers of 6 nm-thick GaAs quantum wells were used as the saturable absorber. The measured modulation depth of the 800 nm SESAM/SBR was 4.5%. The second SESAM/SBR (the 850 nm SESAM/SBR) had a ~50 nm broad reflectivity bandwidth that is centered around 850 nm ($R>99\%$). In this case, twenty-five pairs of $\text{Al}_{0.95}\text{Ga}_{0.05}\text{As}/\text{Al}_{0.17}\text{Ga}_{0.83}\text{As}$ quarter-wave layers were used in the Bragg stack, and one layer of 25 nm-thick GaAs was used as the saturable absorber. The modulation depth for the 850 nm SESAM/SBR was ~2%.

3. Continuous wave lasing results

3.1 Continuous wave lasing efficiency curves, and Findlay-Clay & Caird analysis

This section presents continuous-wave lasing results for the single-mode diode-pumped Cr:Colquiriites. The output power levels are the highest to date from single-mode diode-pumped Cr:Colquiriite lasers. Single-mode diode-pumping results for Cr:LiCAF have been previously reported [21, 24], so Cr:LiCAF results will be included for comparison only.

Figure 2 shows the cw laser output power variation with output coupler transmission for Cr:LiSAF, Cr:LiSGaF, and Cr:LiCAF lasers. All results were obtained at room temperature with an absorbed pump power of ~ 520 mW, corresponding to a total incident pump power of ~ 600 mW. Up to 257, 269 and 266 mW of output power were obtained with Cr:LiSAF, Cr:LiSGaF and Cr:LiCAF lasers, respectively. The optimum output coupling is ~ 1 -3% for all cases, indicating that the resonator losses are very low. Cr:LiSAF has the highest gain among the three media, since lasing could be obtained at higher output coupling levels compared to Cr:LiCAF and Cr:LiSGaF. This is consistent with its larger $\sigma_{em}\tau_r$ value (Table 1). Cr:LiCAF has the lowest gain and low loss optics ($R > \sim 99.99\%$) are required for efficient laser operation. We also note here that Cr:Colquiriites suffer from thermal effects caused by upconversion processes, and thermal load due to upconversion increases with increasing output coupling. Hence, in Fig. 2, part of the observed reduction in output power at high output coupling is due to increased thermal effects. This point will be discussed more in Section 3.3.

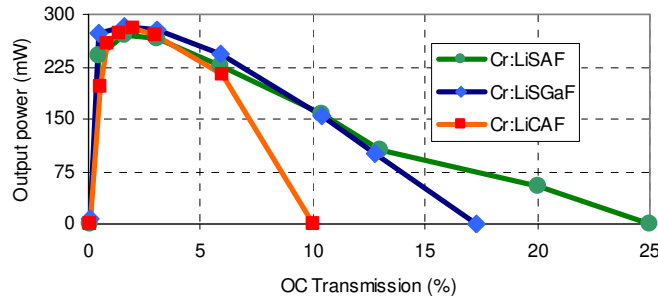


Fig. 2. Variation of cw laser output power with output coupling (OC) for Cr:LiSAF, Cr:LiSGaF and Cr:LiCAF gain media, at ~ 550 mW absorbed pump power.

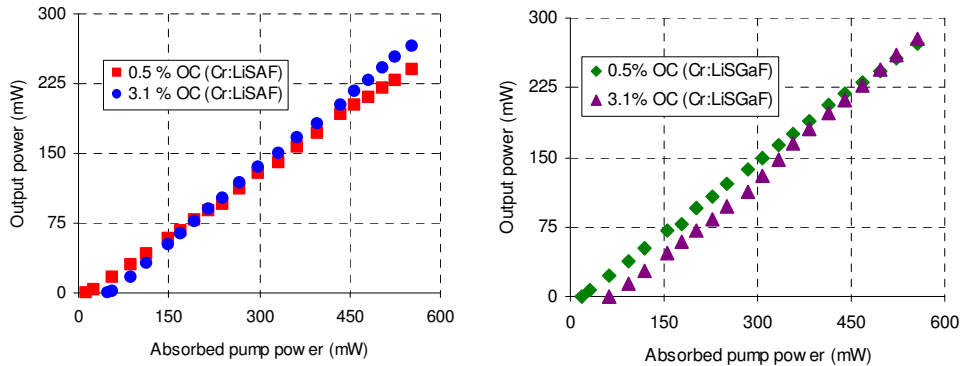


Fig. 3. Cw efficiency curves for the single-mode diode-pumped Cr:LiSAF (left) and Cr:LiSGaF (right) with the 0.5% and 3.1% output couplers. OC: Output coupler.

Slope efficiency data for the Cr:LiSAF laser were measured using nine output couplers ranging from 0.05-25%. Free running cw lasing wavelength was $\sim 835 \pm 10$ nm. Figure 3 (left) shows representative efficiency curves with the 0.5% and 3.1% output couplers. Thresholds as low as 5 mW were measured with the 0.05% output coupler. The highest cw output power (257 mW) was obtained using a 1.6% output coupler while exhibiting a 21 mW lasing threshold and 50% slope efficiency. Slope efficiencies up to 53% were obtained with a 3.1% output coupler. Using the measured threshold pump power with several different output couplers (Findlay-Clay analysis), a roundtrip cavity loss of 0.25% was estimated. Using the measured slope efficiency with different output couplers (Caird analysis), the intrinsic slope efficiency was estimated to be 54%, with roundtrip cavity losses of 0.1%. This intrinsic slope efficiency (54%) is in good agreement with the previously reported value of 53% [2].

For Cr:LiSGaF, the slope efficiency was measured using eight output couplers ranging from 0.05 - 17.5%. Figure 3 (right) shows representative curves with 0.5% and 3.1% output couplers. Similar to Cr:LiSAF, the cw lasing wavelength was $\sim 835 \pm 10$ nm, and thresholds as low as 6 mW were obtained with a 0.05% output coupler. Using the 1.6% output coupler, the highest cw output power (269 mW), a 31 mW lasing threshold and 55% slope efficiency were measured. Slope efficiencies up to 62% were obtained with a 5.9% output coupler. The roundtrip cavity loss was estimated at 0.35% and 0.1% using Findlay-Clay and Caird analyses. Caird analysis yield a value of 60% for the intrinsic slope efficiency, slightly higher than previously reported (52% [3]).

Lastly, for the Cr:LiCAF laser [21, 24], the laser slope efficiency was measured using seven different output couplers ranging from 0.05-10%. The cw lasing wavelength was ~ 790 nm. A threshold as low as 5 mW was measured using a 0.05% output coupler. A 1.95% output coupler gave the highest cw output power (266 mW), with a 43 mW lasing threshold and 54% slope efficiency. Caird analysis yields an intrinsic slope efficiency of 66%, and roundtrip cavity loss of 0.25%. The intrinsic slope efficiency (66%) is in good agreement with the literature (67% [4]).

3.2 Continuous wave laser tuning results

Figure 4 shows the measured cw tuning range for the Cr:Colquiriite lasers at ~ 520 mW absorbed pump power. Record tuning ranges were obtained, which we believe result from increased pump powers, better pump beam quality, low-loss optics, and better quality crystals with lower parasitic loss levels (especially for Cr:LiCAF [21]). Continuous tuning of the Cr:LiCAF laser from 754 to 871 nm was demonstrated using a 400- μm -thick quartz birefringent filter and a 0.5% output coupler (Fig. 4). Higher output powers were obtained using a 1.5% output coupler over a narrower tuning range (756-865 nm). This is the first demonstration of tuning above 840 nm for Cr:LiCAF [4, 21]. We believe that tuning below 754 nm was limited by the strong self-absorption losses of the highly doped crystal. For example, the single-pass absorption of the crystal was measured to be $\sim 3.4\%$ at 750 nm. Previously, Payne et al. demonstrated tuning between 720-840 nm in quasi cw operation using a 0.32 mol.% doped Cr³⁺:LiCAF crystal [4]. The low doping and pulsed excitation (1 ms pulses with 2W of average power) may have enabled the extended short wavelength tuning in [4]. A more detailed discussion on cw tuning limits of Cr:LiCAF can be found in [21].

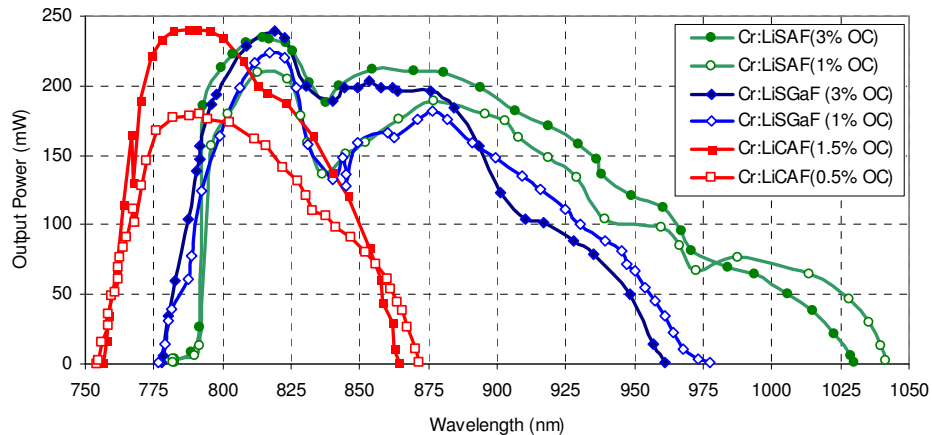


Fig. 4. CW tuning curves for Cr:LiSAF, Cr:LiSGaF and Cr:LiCAF at room temperature, at ~ 520 mW absorbed pump power. Two different output couplers were used.

As mentioned previously, a broadband pump mirror set was used for tuning measurements in the Cr:LiSGaF and Cr:LiSAF lasers, since the narrowband mirrors prevented tuning above ~ 900 nm. Continuous tuning from 777 to 977 nm was demonstrated in the Cr:LiSGaF laser using a 300- μm thick quartz birefringent filter and a 1% output coupler. A

3% output coupler gave similar output powers but slightly reduced tuning range (778-961 nm). Comparing the shape of the tuning curves from the 1% and 3% output couplers, the dip around 835 nm is from leakage in the broadband pump mirrors. To our knowledge, the broadest tuning range of Cr:LiSGaF to date is from ~785 to ~935 nm [9], using a 2 W Kr laser pump. Hence, this study extends the tuning range of Cr:LiSGaF by ~50 nm using inexpensive single-mode diodes for pumping.

Among the Cr:Colquiriite materials investigated, the broadest tuning range was achieved with Cr:LiSAF. In the Cr:LiSAF tuning experiments, tuning was performed using a fused silica prism. With a 1% OC, the Cr:LiSAF laser could be tuned between 782 to 1042 nm. A 3% OC enabled a smoother tuning curve with a slightly narrower range (782-1030 nm). Ti:Sapphire has wide a fractional tuning range of 0.57 (660-1180 nm, $\Delta\lambda/\lambda_0 \approx 0.57$, where $\Delta\lambda$ is the full width of the tuning range and λ_0 is the central wavelength). The fractional tuning ranges are ~0.29 for Cr:LiSAF (780-1042 nm, $\Delta\lambda/\lambda_0 = 262/911$), ~0.23 for Cr:LiSGaF (777-977 nm, $\Delta\lambda/\lambda_0 = 200/877$) and ~0.19 for Cr:LiCAF (720-871 nm, $\Delta\lambda/\lambda_0 = 151/795.5$).

3.3 Investigation of thermal effects

In order to investigate thermal effects on the laser crystals, the cw laser performance was measured at several different crystal holder temperatures using a water re-circulator. Figure 5 shows the cw output powers versus crystal holder temperatures for the Cr:LiSAF and Cr:LiSGaF lasers, at an absorbed pump power level of ~520 mW. For each crystal, the variation of the output power with temperature was measured using two different output couplers to study the effect of output coupling on the thermal load.

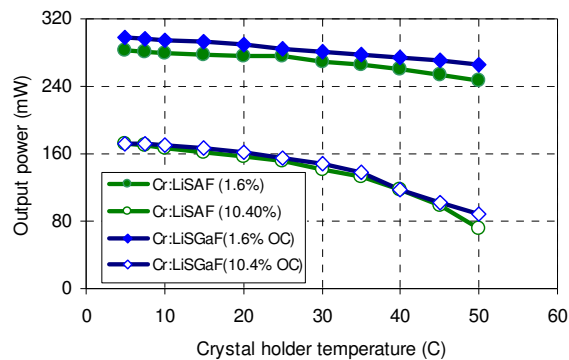


Fig. 5. Variation of cw output power with crystal holder temperature for Cr:LiSAF and Cr:LiSGaF gain media at ~520 mW absorbed pump power using two different output couplers.

Figure 5 shows that, as expected, thermal effects are more severe with the higher 10.4% output coupler, due to increased upconversion-induced heating [21]. However, thermal effects are negligible at room temperature with the 1.6% output coupler (comparing the output powers at 5 and 20 °C). Hence, although there is some thermal loading using Cr:LiSAF and Cr:LiSGaF, water cooling was not required (for operation near the optimum output coupling of 1-3%, cooling the crystal yields only ~5% increase in output). Also, although Cr:LiSGaF has slightly better thermal properties than Cr:LiSAF, thermal effects caused a similar decrease in output power. We believe this is caused by the slightly higher absorption of the 3% chromium-doped Cr:LiSGaF crystal ($\alpha \approx 10.5 \text{ cm}^{-1}$), compared to the 1.5% Cr:LiSAF crystal ($\alpha \approx 9 \text{ cm}^{-1}$). We therefore believe a 2.5% doped Cr:LiSGaF crystal would exhibit better laser performance.

Finally, for the Cr:LiCAF gain medium, the thermal effects were measured using the 1.6% output coupler, and the variation in the output power was very small (1-2 mW). This is expected, since Cr:LiCAF has much better thermal properties as compared to Cr:LiSAF and Cr:LiSGaF (higher thermal conductivity [19], higher $T_{1/2}$ value [7, 18], lower thermal lensing [18], lower quantum defect, lower excited-state absorption [2, 4], and a lower upconversion rate [16], Table 1).

4. Mode Locking results

In the cw mode-locked regime, ~50-100 fs pulses with 1-2.5 nJ of pulse energies (at ~100 MHz repetition rates) were obtained from all of the Cr:Colquiriite materials. Results for Cr:LiCAF have been published [21, 24, 29, 30], and are also included here for comparison. Results with Cr:LiSAF and Cr:LiSGaF will be discussed in more detail below.

4.1 Mode-locking results with Cr:LiSAF

Cr:LiSAF has the highest gain and broadest tuning range among the Cr:Colquiriites. Two different SBR/SESAMs that were designed to operate around 800 nm and 850 nm were used in this study. Table 2 lists some of the key mode-locking results obtained with Cr:LiSAF. Using different configurations, pulses as short as 41 fs, pulse energies up to ~2.2 nJ and average mode-locked output powers up to 187 mW (corresponding to an 8 % electrical-to-optical conversion efficiency) were obtained.

Table 2. Pulse energies, average output powers, and pulse durations from Cr:LiSAF. Repetition rates, central wavelength of spectrum, and dispersion compensation method are also listed.

Pulse energy (nJ)	Output power (mW)	Pulse width (fs)	Repetition rate (MHz)	Central Wavelength (nm)	SBR/SESAM wavelength (nm)	Dispersion compensation method
1.36	156	75	114	850	850	DCMs
1.76	149	46	85	870	850	FS Prism pair
2.2	187	74	85	859	850	FS Prism pair
1.17	144	85	123	812	800	GTI
1.43	121	41	84	814	800	FS Prism pair

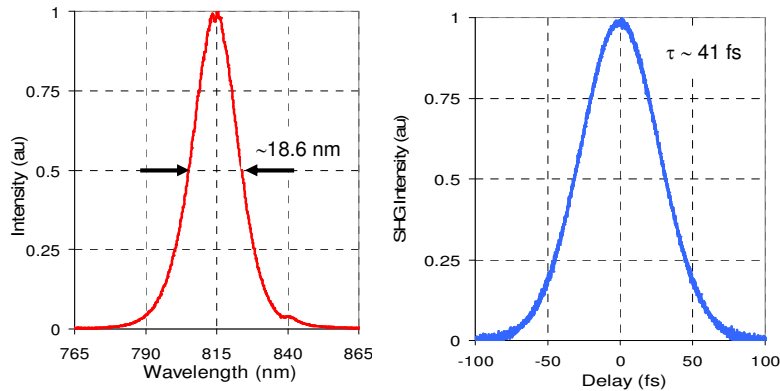


Fig. 6. Spectrum and autocorrelation of the single-mode diode-pumped mode-locked Cr³⁺:LiSAF laser using an 800 nm SBR/SESAM with a 3% OC at ~530 mW absorbed pump power. The autocorrelation FWHM is 63 fs, corresponding to a 41-fs pulse duration (assuming a sech² pulse). The average power is 121 mW, with 1.43 nJ pulse energy at 84-MHz repetition rate. The bandwidth is 18.6 nm (FWHM) at ~814 nm with a ~0.34 time-bandwidth product.

Figure 6 shows an example of the optical spectrum and autocorrelation trace for the 41 fs, 1.43 nJ pulses that were obtained with the Cr:LiSAF laser. The data was taken with a 3% output coupler at an absorbed pump power of ~530 mW. An FS prism pair was used for dispersion compensation and the 800 nm SBR/SESAM was used for mode-locking [Fig. 1 (a)]. The prism separation was ~40 cm, and a 15 cm radius of curvature mirror focused the beam on the SESAM/SBR [M4 in Fig. 1 (a)]. The 5-mm-long, 1.5% Cr-doped Cr:LiSAF crystal (GVD ~22.5 fs²/mm) and intracavity air produced a total GVD of ~300 fs². The estimated total dispersion of the cavity with minimal prism insertion was ~ -250 fs². Tuning the dispersion by adjusting the prism material insertion, resulted in pulses as short as 41-fs (assuming sech² pulses) with 121 mW average power and 18.6 nm bandwidth near 814 nm at

84 MHz (~ 1.43 -nJ pulse energy). The estimated total cavity dispersion to produce the 41-fs pulse was ~ -50 fs². The time-bandwidth product was ~ 0.34 , close to the transform limit of 0.315 for sech² pulses. Note that the spectrum has wings down to 780 nm, which is the cw tuning limit for Cr:LiSAF gain media.

Figure 7 shows a typical efficiency curve, when the cavity contains a SESAM/SBR, showing the output power as well as the different operating regimes. The laser operated in a purely cw regime for absorbed pump powers up to ~ 150 mW. Then Q-switched mode-locked pulses were observed for pump powers between ~ 150 to ~ 250 mW. Finally, for pump powers above ~ 250 mW, stable and self-starting cw mode-locking was obtained. Hence, pumping at full pump-power, the SESAM/SBR mode-locked laser was self-starting and did not Q-switch.

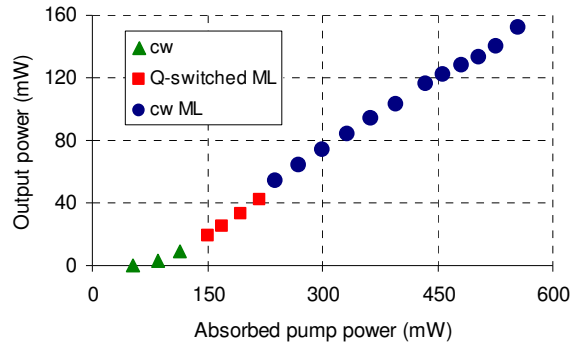


Fig. 7. Representative efficiency curve for the single-mode diode-pumped mode-locked Cr:LiSAF laser, showing different regimes of operation with the SESAM/SBR: cw, continuous-wave; Q-switched ML, Q-switched mode-locked; cw ML, continuous-wave mode-locked operation. The boundary between stable cw mode-locking and q-switched mode-locking depends on the SESAM/SBR incident pulse energy fluence, hence, this curve is a representative example (see [21, 24] for other examples, and [21] for a detailed discussion).

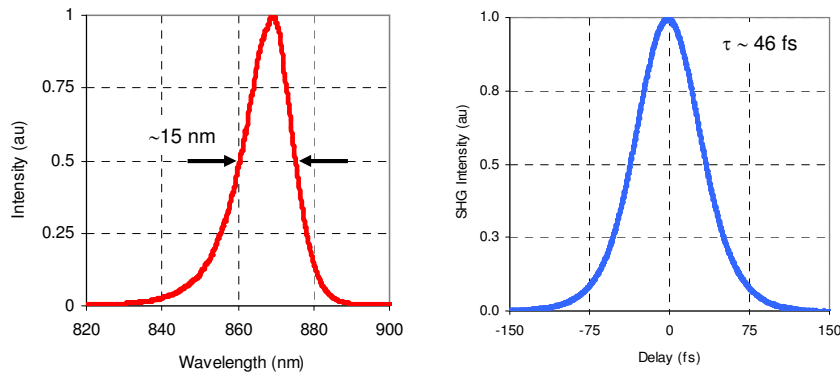


Fig. 8. Spectrum and autocorrelation of 46 fs, 1.76 nJ pulses centered around 870 nm using an 850 nm SBR/SESAM. Average output power was 157 mW with a 3% OCT and 85 MHz repetition rate cavity.

Pulses of 46 fs duration, and 1.76 nJ pulse energy were generated by changing to the 850 nm SBR/SESAM (Fig. 8). Pulses widths could be varied by tuning the intracavity dispersion as shown in Figure 9. Since the spectrum is narrower for longer pulses, the effective loss decreases. For example, for the 74-fs pulses, the average output power increased to 187 mW, with a corresponding pulse energy of 2.19 nJ (Table 2). There is an apparent spectral shift to longer wavelengths with decreasing pulsewidth (with increasing pulse peak power). A similar spectral shift in fs Cr:Colquiriite lasers was observed by Sorokina, et al. and is attributed to the Raman self-frequency shift [11], but further investigation is necessary. Finally, the spectral asymmetry may be partly due to the limited reflectivity band of the SBR/SESAM and the pump mirror, which causes the loss to increase above ~ 880 nm.

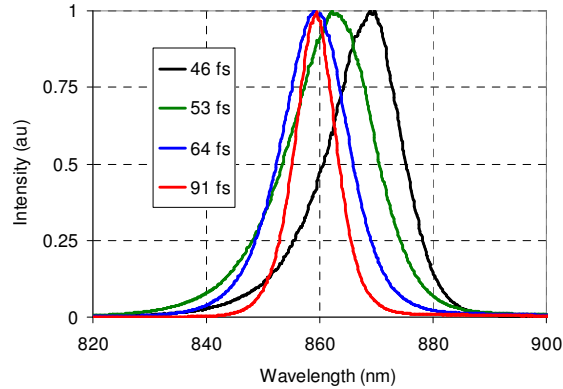


Fig. 9. Spectra of 46, 53, 64 and 91-fs long pulses (assuming sech^2 pulses) from the Cr^{3+} :LiSAF laser. The estimated total cavity dispersion was -30, -110, -190 and -270 fs^2 , respectively. The time bandwidth product was ~ 0.35 for all cases.

4.2 Mode-locking results with Cr:LiSGaF

Results from the Cr:LiSGaF laser were similar to results from the Cr:LiSAF laser. The Cr:LiSGaF laser generated pulse energies as high as ~ 2.3 nJ, and pulsewidths as short as 52 fs (Table 3). Using the two SBR/SESAMs, pulses that were centered around 810 or 860 nm, could be generated. Since the details of the experiments are similar to Cr:LiSAF laser, the discussion will be brief.

Table 3. Summary of cw mode-locking results with Cr:LiSGaF gain media.

Pulse energy (nJ)	Output power (mW)	Pulse width (fs)	Repetition rate (MHz)	Central Wavelength (nm)	SBR/SESAM wavelength (nm)	Dispersion compensation method
1.83	139	55	75	860	850	DCMs
2.0	172	52	86	867	850	FS Prism pair
2.31	186	72	81	815	800	GTI
1.71	147	54	86	820	800	FS Prism pair

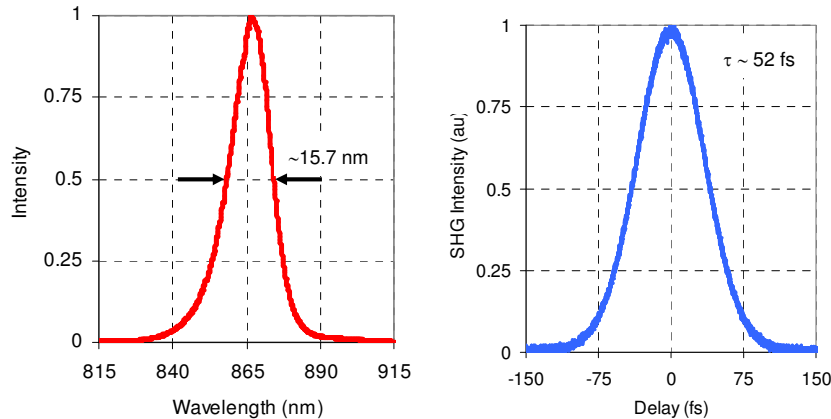


Fig. 10. Spectrum and autocorrelation trace for the 52-fs, 2 nJ pulses from the single-mode diode-pumped Cr:LiSGaF laser, using FS prisms for dispersion compensation and a 850 nm SBR/SESAM. The average output power was 172 mW, at ~ 530 mW absorbed pump power, with a 3% output coupler. The bandwidth was 15.7 nm (FWHM) centered near ~ 867 nm with a ~ 0.33 time-bandwidth product.

Figure 10 show an example of the spectra and autocorrelation using the 850 nm SBR/SESAM, with a 3% output coupler at an absorbed pump power of ~ 530 mW. Dispersion compensation was performed with a FS prism pair separated that was by 42 cm. The 5-mm-long, 3% Cr-doped Cr:LiSAF crystal (GVD ~ 28 fs²/mm) and intracavity air produced a total GVD of ~ 320 fs². A 15 cm radius of curvature mirror focused the beam on the SBR/SESAM. Mode-locking was self-starting, and robust against environmental disturbances. The laser produced 52 fs pulses with 172 mW average power and has a 15.7 nm spectral bandwidth near 867 nm at 86 MHz (~ 2 -nJ pulse energy) with a time bandwidth product of ~ 0.33 . The estimated total cavity dispersion to generate 52-fs pulses was ~ -50 to -100 fs².

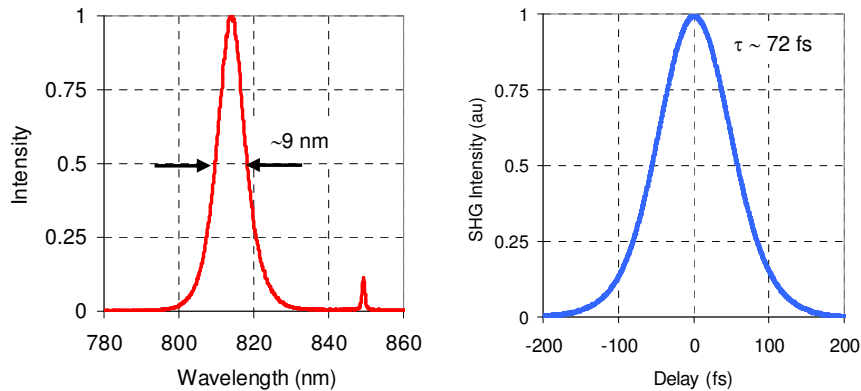


Fig. 11. Spectrum and autocorrelation of 72-fs, 2.31 nJ pulses from the single-mode diode-pumped Cr:LiSGaF laser, using a GTI mirror for dispersion compensation and 800 nm SBR/SESAM. The average output power was 186 mW, at ~ 560 mW absorbed pump power, with a 3% output coupler.

Figure 11 shows a spectrum and autocorrelation for the Cr:LiSGaF laser, using the 800 nm SBR/SESAM, and a GTI mirror for dispersion compensation. The laser generated 72 fs pulses with 186 mW average power and has a 9 nm bandwidth centered around 815 nm, at 81 MHz repetition rate (~ 2.31 nJ pulse energy). The spike in the spectrum around 850 nm is from GVD oscillations of the GTI mirror. GTI mirrors can provide high dispersion in one bounce, enabling compact cavities. Moreover, since the number of bounces required for dispersion compensation is low, the total intracavity loss is minimized. However, GTIs have large GVC oscillations which cause spectral modulation (especially for < 100 fs pulses). Similar spectral modulation was also observed using GTI mirrors with Cr:LiSAF and Cr:LiCAF lasers [30].

4.3 Mode-locking results with Cr:LiCAF

Cr:LiCAF gain medium is distinct in the Cr:Colquiriite family (Table 1). Cr:LiCAF lases in the spectral range from ~ 750 to ~ 800 nm, which is not accessible by the other Cr:Colquiriites and has better thermal properties, which can enable high-power operation. The main disadvantage of Cr:LiCAF is its low emission cross section, which results in low gain (round-trip gain $< 10\%$), requiring extremely low loss optics. Moreover, due to its lower emission cross section, Cr:LiCAF has higher tendency to q-switch [21]. However, despite these disadvantages, 750-800 nm spectral region is important for applications such as amplifier seeding or multiphoton microscopy [29], and the superior thermal properties of Cr:LiCAF can enable power scaling.

Pulse durations of 45 fs were obtained with 120 mW average power at 130 MHz repetition rates, corresponding to 0.9 nJ pulse energies. Pulse energies of 1.8 nJ with 70 fs pulse durations and 180 mW average powers at 100 MHz repetition rates were also generated. Mode-locking was obtained by using the 800 nm SBR/SESAM (the gain was too low at 850 nm for mode-locking with the 850 nm SBR/SESAM (Fig. 4)). The average output powers are slightly lower than from the Cr:LiSAF and Cr:LiSGaF lasers, due to the susceptibility of

Cr:LiCAF to losses (losses from the SBR/SESAM and DCMs). Recently, using an extended cavity Cr:LiCAF laser, pulse energies as high as 15.2 nJ [30], with peak powers exceeding 100 kW were also demonstrated. A detailed description of the mode-locking results with Cr:LiCAF can be found in [21, 24, 29, 30].

4.4 Mode-locking tuning results for Cr:LiSAF

Two SBRs/SESAMs that were designed for 800 nm and 850 nm were used for mode-locking. SESAM/SBRs enable robust and turn-key laser operation of Cr:Colquiriite gain media. However, the narrow bandwidth of standard SESAM/SBRs (~50 nm) limits pulsewidths to the ~40 fs level and limit the tunability of modelocked operation. In this section, we will present our preliminary mode-locking tuning results with the Cr:LiSAF laser.

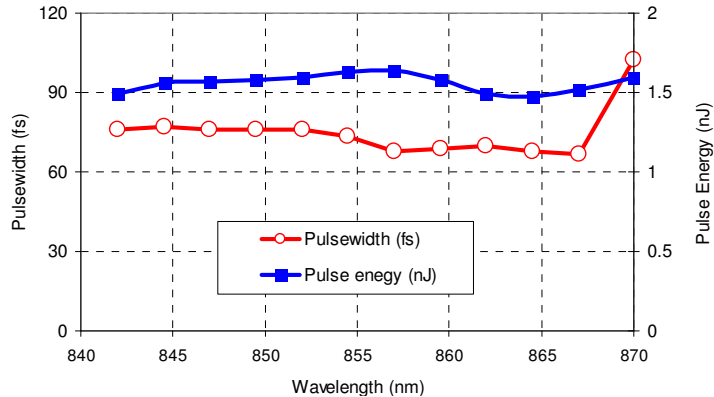


Fig. 12. Tuning data for the modelocked Cr:LiSAF laser. The graph shows the variation of the pulsewidth and energy as a function of the laser central wavelength.

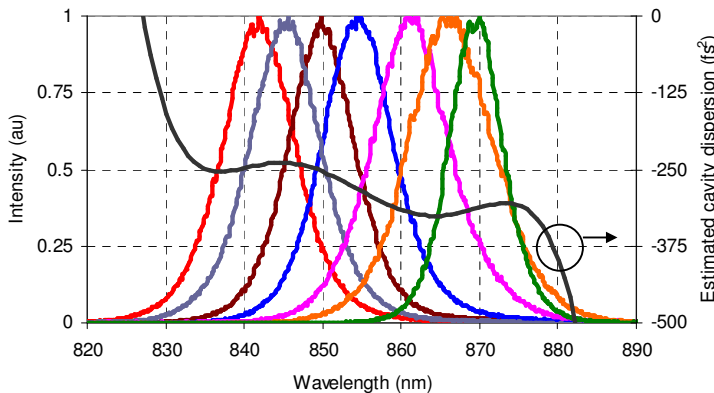


Fig. 13. Sample spectra from the Cr³⁺:LiSAF laser, showing the tunability of the central wavelength of the laser from 842 nm to 870 nm, for the sub-80-fs pulses. Estimated total cavity dispersion is also shown.

Figure 12 shows the measured variation of the pulse energy and the pulsewidth as a function of the central wavelength of the pulse for ~sub-80-fs pulses. The central wavelength could be tuned continuously from ~842 nm to ~870 nm (~28 nm tuning), by rotating the birefringent filter element (the data in Fig. 12 was taken at discrete wavelengths separated by ~2.5 nm). Custom designed DCM mirrors were used and the total cavity dispersion was estimated at -300 fs² (Fig. 13). The pulses were generated with a 3% output coupler, and with ~530 mW absorbed pump power using the 850 nm SESAM/SBR. The pulsewidth was <80 fs and average output power was ~126 mW and remained almost constant along the full tuning bandwidth. The laser repetition rate was 81.6 MHz and pulse energies were ~1.55 nJ.

Figure 13 shows sample optical spectra for the sub-80-fs pulses, along with the estimated total cavity dispersion. The dispersion estimate uses 1 SESAM/SBR reflection, 10 DCM reflections, ~ 3.6 m of intracavity air, 10 mm of Cr:LiSAF crystal and 6 mm of quartz birefringent plate. The relatively large fluctuation in the GVD curve is mostly due to the SESAM/SBR, which had large GVD deviations from 0 fs^2 away from the central wavelength (850 nm). We believe the limited GVD bandwidth of the SESAM/SBR restricted the tuning range to ~ 28 nm. The output power remained nearly constant even at the edges of the tuning range, suggesting that the SESAM/SBR reflective bandwidth, and the roll off in Cr³⁺:LiSAF gain did not limit the tuning within this range. When the central wavelength was tuned above 870 nm, a cw peak appeared around ~ 880 nm. Appearance of this cw peak is expected because of the sharp dispersion variation beyond ~ 875 nm (Fig. 13). When the central wavelength was tuned below ~ 840 nm, the laser operated in the Q-switched mode-locked regime. We believe this is due to the increased dispersion beyond ~ 835 nm, which prevents mode-locking.

Increasing the negative dispersion of the cavity to $\sim -600 \text{ fs}^2$ resulted in the generation of ~ 140 fs pulses and enabled slightly broader tuning. The laser was tunable over 33.2 nm, from 832.5 nm to 865.7 nm and generated ~ 140 fs pulses with ~ 142 mW average power at a 86.3 MHz repetition rate (~ 1.64 nJ pulse energy). Doubling the intracavity dispersion level from $\sim -300 \text{ fs}^2$ to $\sim -600 \text{ fs}^2$ level roughly doubled the pulsewidths, which increased from ~ 75 fs to ~ 140 fs as expected from soliton mode locking. We believe that for the ~ 140 fs pulses, the tuning range was restricted both by the reflectivity and GDD bandwidth of the SESAM/SBR.

In the tunable mode-locking experiments, tuning was performed only by rotating the birefringent plate, without adjusting other laser elements. The pulsewidths and pulse energies remained almost constant throughout the full tuning range. A slightly broader tuning range from ~ 825 nm to ~ 875 nm was previously reported using a multimode diode pumped Cr:LiSAF laser, mode-locked using a high-finesse antiresonant Fabry–Perot SESAM/SBR which had a slightly broader reflectivity bandwidth (~ 60 nm) than the SESAM/SBRs that was used in this study [31]. Tuning was performed using an SF10 prism pair and slit which required dispersion adjustment and caused variations in the pulsewidth ($\sim 50 - 200$ fs) with tuning. Broad tuning ranges are possible with KLM mode locked Cr:LiSAF lasers [32, 33], but it is difficult to obtain long-term stable and robust mode-locked operation. Using two tapered diode lasers with 500 mW diffraction limited output, 809-910 nm tuning with ~ 100 fs, ~ 1 nJ pulses has been demonstrated [33].

Compared with the cw tuning range demonstrated in this work for Cr:LiSAF (~ 780 -1040 nm), mode-locked tuning bandwidths are significantly narrower. This is a significant limitation for applications which require broadly tunable fs pulses. Ti:Sapphire has a higher nonlinear index, enabling long term stable and robust KLM operation. Because KLM is not wavelength dependent, the tuning range for cw mode-locking (680 to 1080 nm) in Ti:Sapphire approaches the cw tuning range (675 to 1100 nm).

Although standard SESAMs/SBRs have ~ 50 nm reflectivity bandwidth, broadband SESAMs/SBRs can have bandwidths of several hundred nm [34, 35]. With future progress in broadband SESAM/SBR technology, mode-locked Cr:LiSAF lasers have the potential to generate sub-100-fs pulses with a tunability from ~ 800 nm to ~ 1000 nm [34, 35].

5. Summary and discussion

We have demonstrated efficient cw and cw mode-locked operation of Cr:Colquiriite lasers that are pumped by inexpensive single-mode AlGaInP laser diodes. In cw lasing experiments, output powers up to ~ 270 mW and slope efficiencies up to 62% were demonstrated. The cw tuning range of different Cr:Colquiriite crystals covers the wavelength range from 754 to 1042 nm. Mode-locking using standard SESAM/SBRs generates ~ 50 -100 fs pulses with ~ 1 -2.5 nJ of pulse energy from 100 MHz repetition rate cavities. A recent study has shown that pulse

energies can be scaled up to ~15 nJ using extended cavities [30]. Mode-locked tuning from 842-870 nm was demonstrated at 80 fs pulse durations and was limited by the SESAM/SBR.

Among the Cr:Colquiriites, Cr:LiSAF has the highest gain and broadest tuning range, making it attractive over Cr:LiSGaF and Cr:LiCAF (Table 1). Cr:LiSGaF, has slightly better thermal properties, slightly higher intrinsic slope efficiency and slightly higher nonlinear refractive index as compared to Cr:LiSAF; however, these advantages may not be sufficient to offset the disadvantages from lower gain. Cr:LiCAF is distinct from Cr:LiSAF and Cr:LiSGaF. The main advantage of Cr:LiCAF is its blue-shifted emission spectrum covering ~750 to ~800 nm. This spectral region is quite important for applications like Ti:Sapphire amplifier seeding and multiphoton microscopy. Moreover, the thermal properties of Cr:LiCAF are superior to other Cr:Colquiriites; hence it can enable better power scaling.

In summary, we have presented single-mode diode-pumped Cr³⁺:Colquiriite lasers as an attractive, low-cost alternative to Ti:Sapphire. Cr:Colquiriite lasers should be lower cost compared to Ti:Sapphire technology since they use low cost laser diodes as the pump source, enabling the total cost of materials to be reduced below ~\$10k. Cr:Colquiriite lasers have high electrical-to-optical conversion efficiencies (~10%), and can be used in applications where minimal power consumption is critical. In addition, Cr:Colquiriite technology can be made compact and portable, since the diodes and the laser crystal require no water cooling and the diodes can be run by batteries. SESAM/SBRs enable turn-key modelocked operation and should be suitable for use outside the research laboratory environment. Broadband tunable femtosecond pulse generation is limited by SESAM/SBR bandwidth and requires further development. However, the low cost and high performance of diode pumped Cr:Colquiriite gain media have the potential to replace Ti:Sapphire technology for selected applications in nonlinear optics, pump probe spectroscopy, amplifier seeding, and multiphoton microscopy.

Acknowledgements

We thank Peter Fendel and Hyunil Byun for experimental help and acknowledge support by the National Science Foundation (BES-0522845), Air Force Office of Scientific Research (FA9550-07-1-0014 and FA9550-07-1-0101), National Institutes of Health (2R01-CA075289-12 and 5R01-NS057476-02) and Thorlabs, Inc.